

Predicting ICME Signatures at L1 with a Data-Constrained Physical Model

Phillip Hess and Jie Zhang

School of Physics, Astronomy and Computational Sciences
George Mason University
4400 University Dr. Fairfax, VA

Naval Research Laboratory
06/23/2015



- 1 Introduction
- 2 Observations and Events
- 3 Models and Fittings
- 4 Prediction Results
- 5 Discussion
- 6 Conclusions

Introduction

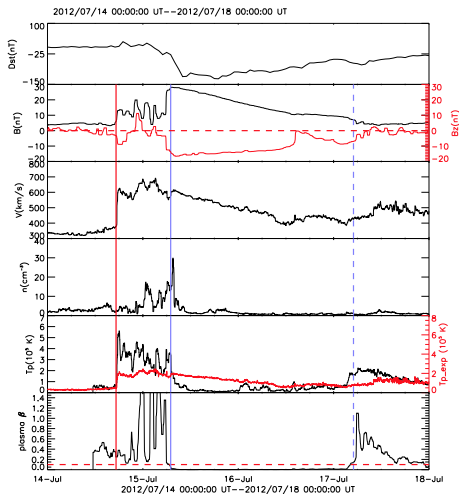
- Coronal Mass Ejections (CMEs) are a significant driver of space weather at the Earth
- An accurate prediction of the arrival of CMEs can help mitigate the harmful consequences associated with a CME
- Currently, the standard of prediction is on the order of about 6 hours Colaninno et al. (2013); Gopalswamy et al. (2013); Möstl et al. (2014); Vršnak et al. (2014)

Our Model

- We present a modified drag-based empirical model to accurately predict the arrival of ICME structures at the L1 point
- For a 7 event sample, we are able to predict arrivals within 4 hours for separate ICME signatures
 - Ejecta- Eruptive material from the corona, likely a flux rope.
 - Sheath- Solar wind plasma accumulated as ejecta propagates. The front of the sheath may or may not be a shock

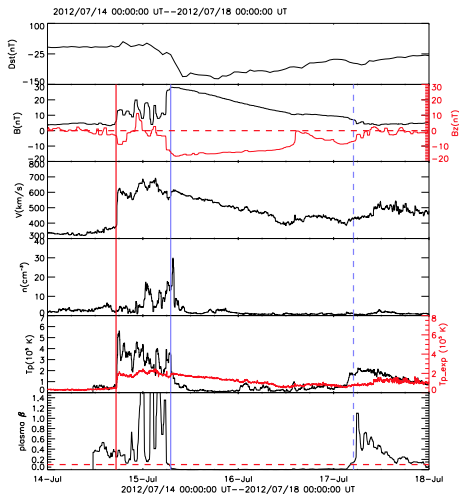
Event Selection

- Events were initially selected from ACE data
- An automatic detection algorithm identified potential ICMEs
- Manual conformation provided a larger list of events, 7 of which were picked based on quality of observations



Determining In-Situ Signatures

- With complex ejecta, there can be ambiguity in where the flux rope or flux rope-like structure passes the observer
- In a normal MC, it is usually easy to determine the boundaries of the flux rope. For complex events, to remain consistent we focus on plasma- β
- The sheath is generally more obvious



Event List

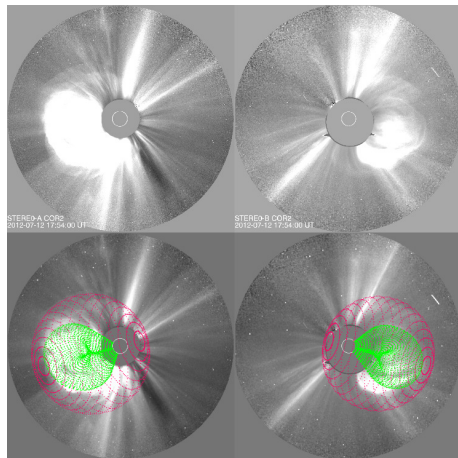
First Measurement ^a	SH Arrival ^b	EJ Arrival ^b	Direction ^c	V_0^c	V_{sw}^d	R_0^e	R_f^e	AR ^f	Flare ^g	Flare Peak ^g
04/03/2010 10:24	04/05 08:00	04/05 11:30	E06S26	854.7	512.4	5.5	62.8	11059	B7	04/03 09:54
05/24/2010 14:54	05/28 02:00	05/28 07:00	E28N03	605.7	362.3	4.6	45.0	-	-	-
09/14/2011 00:24	09/17 02:00	09/17 19:00	W20S16	519.5	396.9	5.3	28.1	11289	-	-
07/12/2012 16:54	07/14 17:00	07/15 07:15	W00S09	1492.0	353.7	4.3	76.6	11520	X1	07/12 15:36
09/28/2012 00:24	09/30 23:00	10/01 06:00	E28N17	1230.5	310.4	6.3	74.1	11577	C3	09/28 00:00
10/27/2012 17:24	10/31 15:00	11/01 00:00	E12N12	400.1	289.8	6.2	49.0	-	-	-
03/15/2013 07:24	03/17 15:30	03/18 00:00	W24S07	1220.2	429.3	7.4	37.0	11692	M1	03/15 05:46

- Table :** a- The time step of the first SECCHI and LASCO images used for GCS fitting. Given the time offsets between the different satellites, the time given refers to the SECCHI observations
 b- Sheath and Ejecta arrivals at ACE as manually determined
 c- Initial Velocity (km/s) is obtained by performing a fit of the data using the drag based model over all observations
 d- Solar wind speed (km/s) is determined by taking an average value of the ACE data preceding the arrival of the sheath signature
 e- The measured ejecta height (R_{\odot}) of the first and last point used for fitting
 f- Associated Active Region given by tracking CME back to the surface using EUV data. Not all CMEs can be linked with an active region
 g- Flare Strength and Peak determined by comparing the EUV observation to X-Ray flux from GOES

Imaging the Events

- The bulk of the imaging for the events is from SOHO-LASCO and STEREO-SECCHI
- The events are all measured as far as possible. For most this means about half the SECCHI HI-1 FOV
- While the CME is still into the LASCO C2/C3 FOV, the three distinct viewpoints are combined
- This multiple viewpoint imaging allows for a 3-D reconstruction of each event

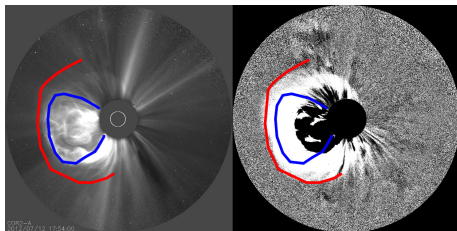
Measuring the Fronts



- Height measurements were based on the raytrace method (Thernisien et al., 2006, 2009)
- Each structure has a unique geometry (Hess & Zhang, 2014)
 - Ejecta- GCS
 - Sheath- Spheroid

Processing the Images

- Different image processing techniques are used
- The front of the sheath can be best observed by using running difference images
- Ejecta boundary can be seen as a bright feature utilizing base ratio images
- The sheath can be seen well into the heliosphere, but as the ejecta propagates and expands, its density drops and becomes fainter



Drag-Based Model

CME measurements are then fit with Drag-Based Model (Vršnak et al., 2013)

$$a(t) = -\Gamma(v(t) - v_{sw})|v(t) - v_{sw}|$$

$$v(t) = \frac{v_0 - v_{sw}}{1 + \Gamma(v_0 - v_{sw})t} + v_{sw}$$

$$R(t) = \frac{1}{\Gamma} \ln[1 + \Gamma(v_0 - v_{sw})t] + v_{sw}t + R_0$$

Initial height (R_0) and velocity (v_0) can be determined reliably from the measurements. Upstream solar wind speed (v_{sw}), ACE data is used for now. This leaves the drag parameter (Γ) as the only true unknown

Modifying the DBM

- Most work using the DBM uses static, fixed parameters
- Making some physical and geometric assumptions about the flux rope, we simplify the form of Γ given by Cargill (2004)

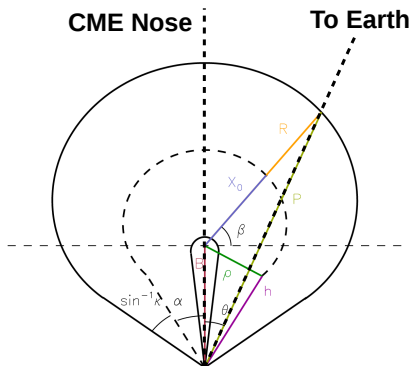
$$\Gamma = \frac{c_d A \rho_{sw}}{M + M_v} \rightarrow \Gamma(R) = \frac{c_d}{\frac{\rho_0 \kappa R_0}{\rho_{sw0}} + \frac{\kappa R}{2}}$$

- Using measurement and fittings, a height-dependent Γ can be determined, yielding an iterative drag model

$$R(t+1) = \frac{1}{\Gamma(R(t))} \ln[1 + \Gamma(R(t))(v(t) - v_{sw})t] + v_{sw}t + R(t)$$

Geometric Correction

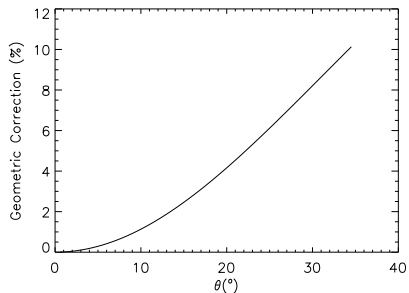
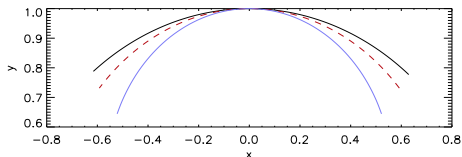
- Initially Predictions for CMEs far from Sun-Earth line were consistently early
- CME curvature effect
- Using the GCS geometry (right) a height correction was determined as a function of the deviation angle (θ)



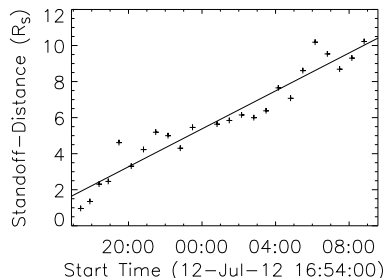
Geometric Correction Cont.

This led to an opposite effect with the GCS geometry causing late predictions, so a weighted average of the two is used

$$h_f = .645h_N + .355h_G$$

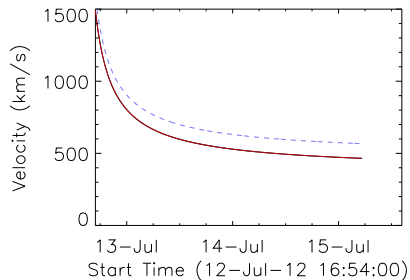
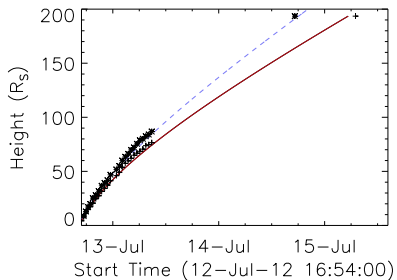


Fitting the Sheath Front



- The previous slides apply to the ejecta
- The method failed to predict the sheath
- By measuring both fronts, the standoff distance in the heliosphere can be known
- Combining the results of a SD fit with the flux rope model gives sheath height

Model Example



Results Table

ICME Date ^a	ΔT_{SF}^b	ΔT_{EJ}^b	ΔV_{SF}^c	ΔV_{EJ}^c	$\rho_{ratio}(R(0))^d$	$\rho_{ratio}(L1)^d$	$\rho_{ratio}(ACE)^e$
04/05/2010	1.89	0.38	23.3	26.4	32.17	0.91	0.41
05/24/2010	5.69	2.52	96.3	38.1	6.70	0.15	1.21
09/14/2011	6.68	4.39	15.8	13.0	3.24	0.09	0.71
07/12/2012	0.84	1.51	24.8	22.4	18.61	0.41	0.61
09/28/2012	0.34	0.9	61.6	45.6	10.31	0.31	0.97
10/27/2012	4.99	0.28	24.5	19.0	14.78	0.47	0.67
03/15/2013	3.91	0.26	22.9	7.2	5.98	0.21	0.38
Average	3.47	1.46	38.5	24.5	13.11	0.36	0.80
RMS	1.58	0.76	17.9	12.9	-	-	-

Table : a- The date of the ICME arrival at ACE

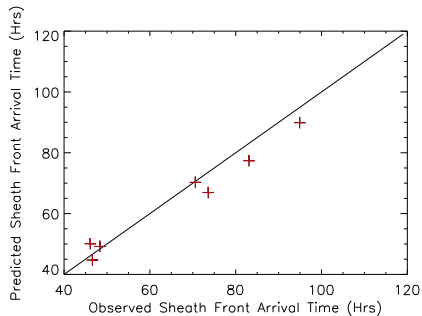
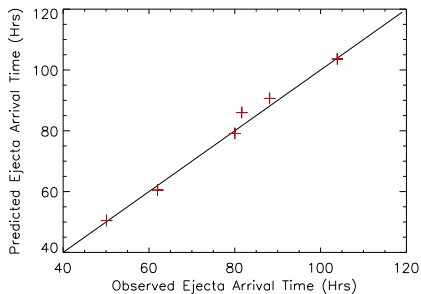
b- The absolute value of the difference in hours between the predicted and observed arrival of the sheath (SF) and Ejecta(EJ)

c- The difference in velocity in km/s between the speed of each feature as predicted by the model and as compared to the average speed observed for each feature in-situ

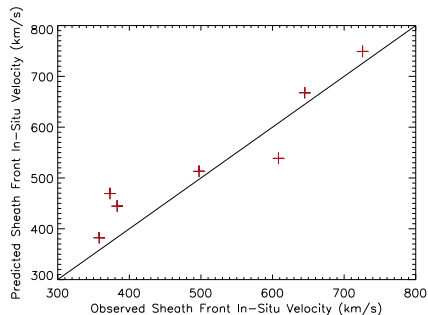
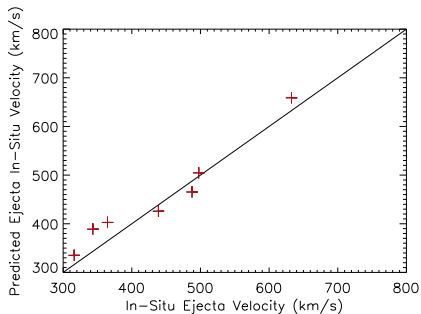
d- The derived density ratio from the model at the initial height of observation and at the point where the ejecta reaches L1

e- The ratio of the densities of the ejecta and solar wind, as determined from the average values of each from ACE.

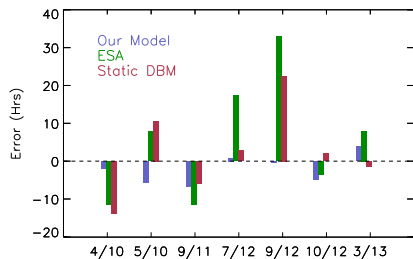
Arrival Comparisons



Velocity Comparisons



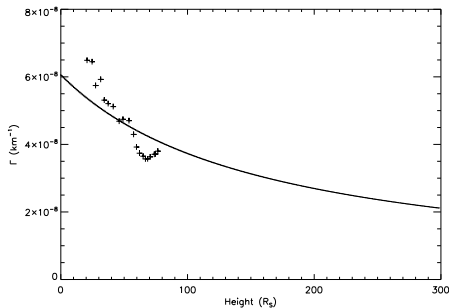
Comparison with Other Models



ICME Date	Our Model	ESA ^a	Static ^b DBM
04/05/2010	-1.9	-11.6	-14.0
05/24/2010	-5.7	7.9	10.6
09/14/2011	-6.7	-11.5	-6.0
07/12/2012	0.8	17.4	2.9
09/28/2012	-0.3	32.9	22.5
10/27/2012	-5.0	-3.7	2.1
03/15/2013	3.9	8.0	-1.4
Abs. Average	3.5	13.3	8.5
RMS	1.6	6.0	4.2

a-Gopalswamy et al. (2013) b-Vršnak et al. (2014)

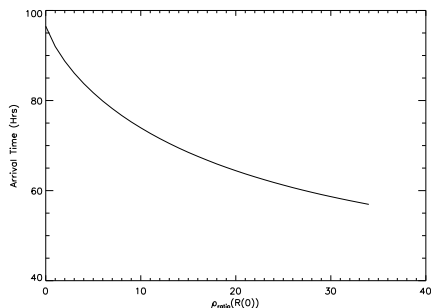
Constraining Γ



- To determine Γ in the model, fittings are performed to each subset of measurements
- The first fittings are to points (0:4), then (0:5) and so on
- This provides an average Γ value out to each point
- Due to the limited number of points and the high variability of Γ , there is often a lot of scatter to these Γ values
- These Γ values are still able to constrain the initial Γ , which is all we need to create our height-dependent Γ profile.

Constraining Γ II

- The Γ values scale to the initial density ratios, which range from 3-32
- To reasonably determine these initial density ratios, a minimum of 5-6 points are needed
- We also test the sensitivity to initial conditions with a hypothetical CME, differing with varying initial density



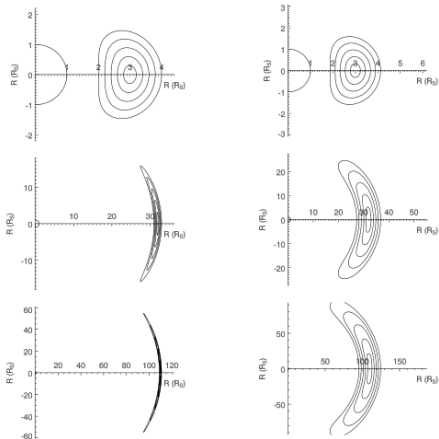
CME Expansion and Density Evolution

- The evolution of CME density relative to the ambient is an important difference in our model
- A constant- Γ drag is based on assuming $\rho \propto 1/r^2$
- This would be valid if CME only expanded with the solar wind and underwent no internal expansion
- Near the Sun, the CME is more dense than the solar wind, but by the time it reaches L1 it is less
- Therefore it stands to reason that the CME must undergo a more rapid drop in density

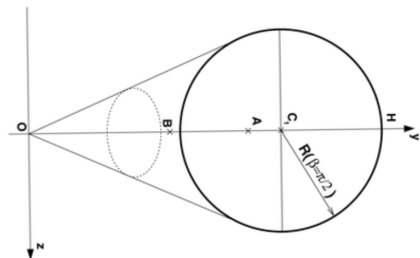
CME Expansion and Density Evolution II

- CME Mass is conserved, so the controlling factor for density is the CME Expansion
- For expansion to be self-similar (GCS), the internal radial expansion would have to equal the lateral expansion in the solar wind
- This would lead to $\rho \propto 1/r^3$
- However, we know CME self-similarity is an over-simplification that breaks down as the CME propagates

Expansion



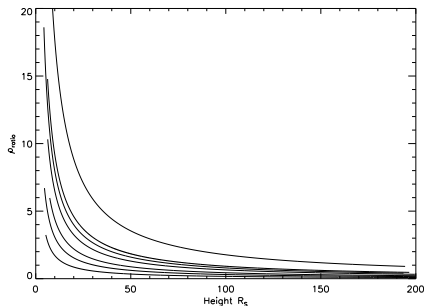
Riley & Crooker (2004)



Thernisien et al. (2009)

CME Expansion and Density Evolution III

- Our model is based on this r^{-3} dependence, leading to the $1/r$ term in Γ
- This model leads to densities that are too low relative to the ambient in-situ
- Based on our curvature analysis, we can estimate the lateral expansion is twice as large as the internal expansion
- This indicates that a density evolution on the order of $r^{-2.4}$ might be more physically accurate for the model



Limitations for Real-Time Operational Forecasting

- Real-time measurement
- Current Lack of STEREO
- Difficulty of Solar Wind Prediction
- Need to test for false positives

Weaknesses of the Model

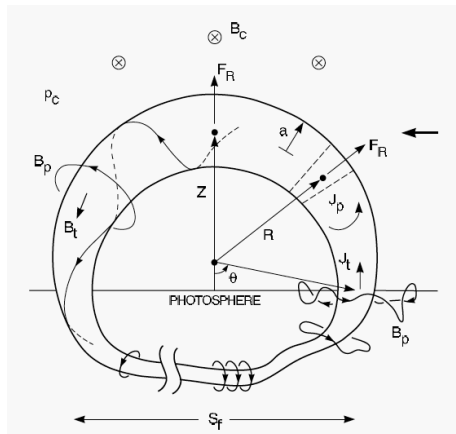
- Multiple CME Interaction Events
- Lack of Magnetic Field Inputs
- The model is only as good as the measurements taken
- Possible Selection Bias

The Advantages of the Model

- Instantaneous Model Calculation
- Maximum Lead Time
- With each piece of new data, new calculation can be run
- The full characteristics of propagation between the Sun and the Earth can be determined

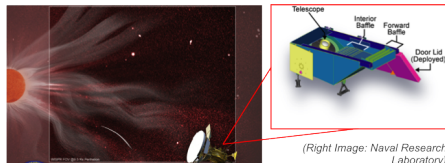
Planned Future Studies

- Testing model with less ideal data (Solar Wind models, realtime data, LASCO only etc.)
- Using White-Light images to estimate CME density near the Sun
- Comparison with other models, such Eruptive Flux Rope (EFR) model (right) (Chen, 1996) for magnetic field
- Better determination of physics of sheath front generation to improve that part of the model

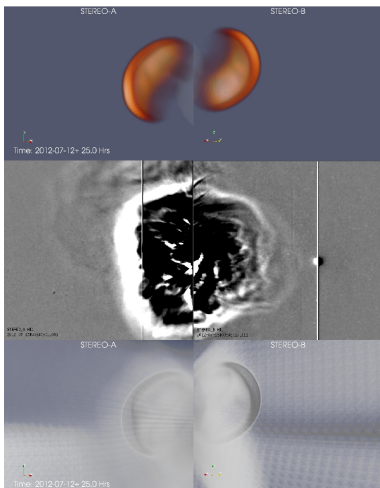


Improvements Based On Future Observations

- With Solar Orbiter and Solar Probe, we will be able to get both extra height and velocity measurements near the Sun
- We can also more accurately determine near Sun densities, which will allow us to include a more physically accurate density/expansion model
- For permanent stereoscopic imaging, a permanent L5 observer would be a great benefit to our tracking process



Work with MHD Models

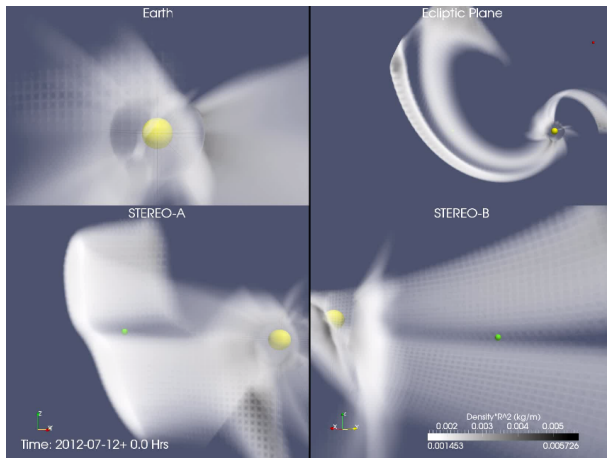


- We have done preliminary work with multiple MHD models
 - COIN-TVD (Shen et al., 2014)
 - ENLIL (Odstrčil & Pizzo, 1999)
- Cross-validation with numerical models allows us to test many physical aspects of our work
- We can also experiment with different inputs in the same model to see how things change
- We can compare visualizations of the MHD model data to real observations and measurement

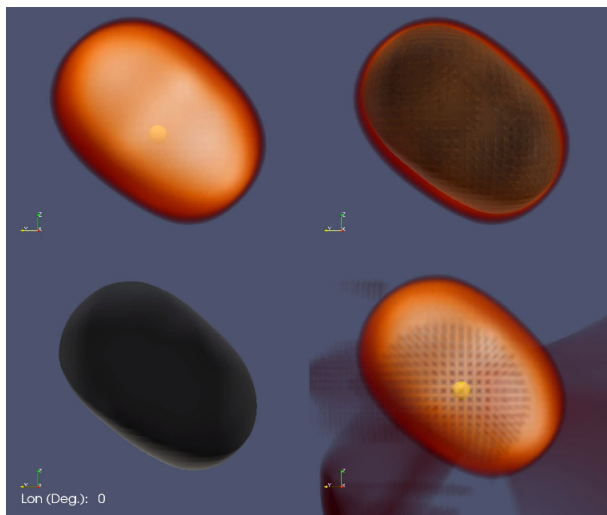
Synthetic COIN-TVD Images



ENLIL data from multiple viewpoints



Effect of Longitude on ENLIL Visualizations



Conclusions and Future Work

- Despite the obstacles, we demonstrate an effective proof of concept
- Our model can also lead to a better physical understanding of CME propagation
- We also demonstrate the importance of considering propagation deviation and considering the unique environment of each eruption
- Better physics/assumptions may still improve the model

ISEST Wiki

- At George Mason, I have worked on the International Study of Earth Affecting Solar Transients (ISEST)
- ISEST is an international collaboration for studying geoeffective CMEs
- Anyone can see the progress of the program, as well as contributed data and a repository of events at the ISEST Wiki Site
<http://solar.gmu.edu/heliophysics>
- Anyone can also create an account at this site and contribute their own commentary, data or events to the site

Thank You

References

- Cargill, P. J. 2004, *Sol. Phys.*, 221, 135
- Chen, J. 1996, *JGR*, 101, 27499
- Colaninno, R. C., Vourlidas, A., & Wu, C. C. 2013, *JGR*, 118, 6866
- Gopalswamy, N., Mäkelä, P., Xie, H., & Yashiro, S. 2013, *Space Weather*, 11, 661
- Hess, P. & Zhang, J. 2014, *ApJ.*, 792, 49
- Möstl, C., Amla, K., Hall, J. R., Liewer, P. C., De Jong, E. M., Colaninno, R. C., Veronig, A. M., Rollett, T., Temmer, M., Peinhart, V., Davies, J. A., Lugaz, N., Liu, Y. D., Farrugia, C. J., Luhmann, J. G., Vršnak, B., Harrison, R. A., & Galvin, A. B. 2014, *ArXiv e-prints*
- Odstrčil, D. & Pizzo, V. J. 1999, *JGR*, 104, 483
- Riley, P. & Crooker, N. U. 2004, *ApJ.*, 600, 1035
- Shen, F., Shen, C., Zhang, J., Hess, P., Wang, Y., Feng, X., Cheng, H., & Yang, Y. 2014, *JGR*, 119, 7128
- Thernisien, A., Vourlidas, A., & Howard, R. A. 2009, *Sol. Phys.*, 256, 111
- Thernisien, A. F. R., Howard, R. A., & Vourlidas, A. 2006, *ApJ.* 652, 763